

**GEOTECHNICAL ASPECTS OF
THE EARTHQUAKE GROUND MOTIONS
RECORDED DURING
THE 1999 CHI-CHI EARTHQUAKE**

by

I. M. Idriss and N. A. Abrahamson

Invited Paper

Keynote Session C

International Workshop on the
Annual Commemoration of the
Chi-Chi Earthquake

September 18-20, 2000

Taipei, Taiwan



GEOTECHNICAL ASPECTS OF THE EARTHQUAKE GROUND MOTIONS RECORDED DURING THE 1999 CHI-CHI EARTHQUAKE^(a)

I. M. Idriss

*Department of Civil & Environmental Engineering, University of California
Davis, California – e-mail: imidriss@aol.com*

N. A. Abrahamson

*Geosciences Group, Pacific Gas & Electric Co.
San Francisco, California – e-mail: naa3@earthlink.net*

Abstract

The earthquake ground motions recorded during this earthquake are examined in terms of the peak horizontal accelerations and peak horizontal velocities recorded at three generalized site conditions. The data suggest a dependence of these parameters on local site conditions; this dependence appears similar to that observed in previous earthquakes, such as the 1971 San Fernando earthquake. Examination of the spectral shapes at the stiffest site category indicates that these sites exhibit nonlinear behavior at the levels of shaking examined (0.3g, 0.4g and 0.7g). Finally, the peak horizontal accelerations recorded in this earthquake are compared to those calculated using attenuation relationships that had been derived prior to this earthquake. These comparisons indicate that the values recorded during the Chi-Chi earthquake are: (i) about 30% of the calculated values at distances less than about 4 km from the rupture surface; (ii) about 70% of the calculated values at distances ranging from about 4 to 20 km; (iii) almost identical to the calculated values at distances ranging from about 20 to 40 km; and (iv) about 50% of the calculated values at distances greater than about 40 km.

These preliminary findings suggest the need to investigate the subsurface conditions at as many of the recordings stations as possible to finalize the site categories and to confirm or modify the findings reached herein. The recordings obtained in the larger aftershocks need to also be examined to provide further information about the differences in the motions recorded during the Chi-Chi earthquake and those obtained in other earthquakes.

^(a) *Proceedings, International Workshop on the Annual Commemoration of the Chi-Chi Earthquake, C-H Loh & W-I Liao, Editors, National Center for Research on Earthquake Engineering (NCREE), Taipei, Taiwan, September 18-20, 2000, Volume III, pp 9 – 22*

Introduction

The Chi-Chi earthquake occurred on the Chelungpu fault on September 21, 1999; the moment magnitude of the main shock was 7.6. The motions generated by the main shock of this earthquake were recorded at the 387 strong motion stations shown in Fig. 1; the recordings from the main shock were made available shortly after the earthquake (Lee et al, 1999). The local site condition at each recording station was estimated based on examining the station location on geologic map of Taiwan. The four generalized site categories listed in Table 1 were defined by Cheng and Lee (2000), who also assigned a site category to each station by locating the recording stations on a geologic map.

Table 1 Site Categories at Strong Motion Stations
(After Cheng and Lee, 2000)

Category	Generalized Description	Generalized Geologic Designation
B	Rock or Rock-Like	Miocene and pre-Miocene
C	Stiff Soil	Pliocene to Pleistocene
D	Soil (other than C or E)	Late-Pleistocene to Recent
E	Soft Soil	Late-Pleistocene to Recent

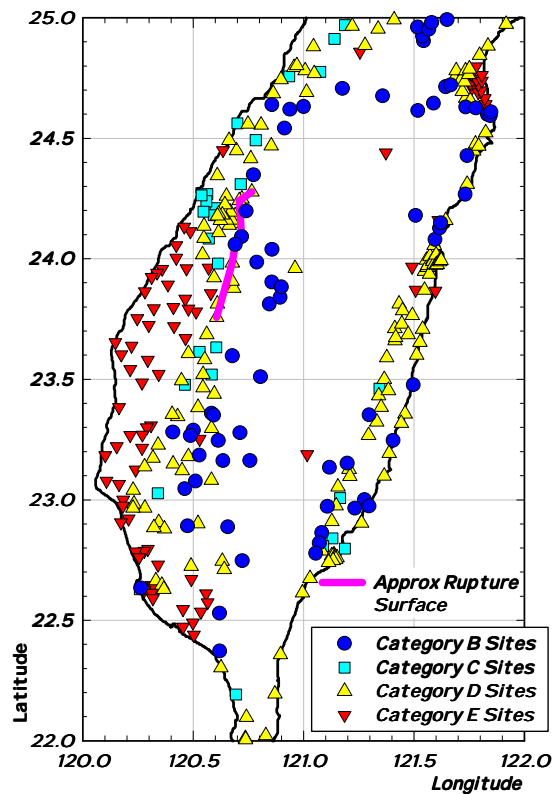


Fig. 1 Locations of Strong Motion Recording Stations in Taiwan

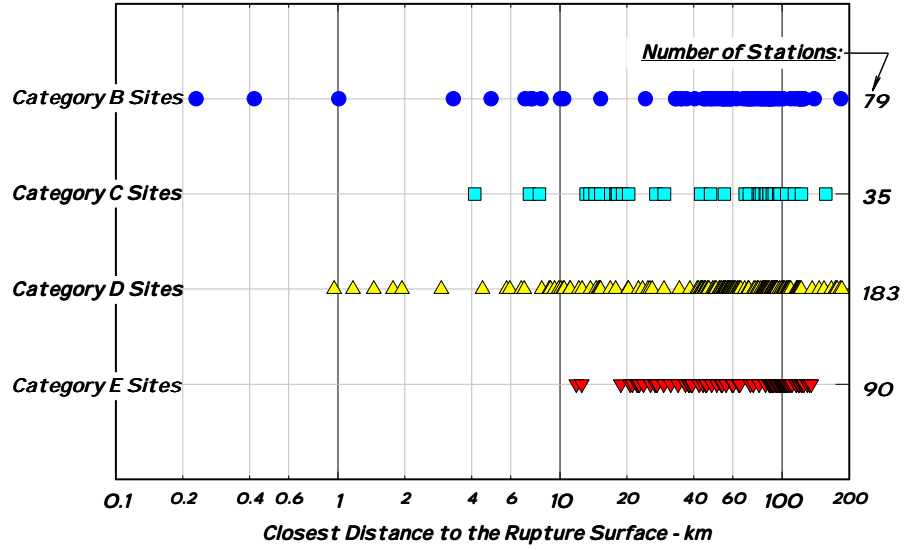


Fig. 2. Fig. 2 Distribution of Strong Motion Recording Stations in Terms of Site Category and Distance from the Rupture Surface

The number of stations for each site category is shown in Fig. 2 as function of distance. The geometric mean of the peak horizontal accelerations and horizontal velocities at each station are presented in Fig. 3.

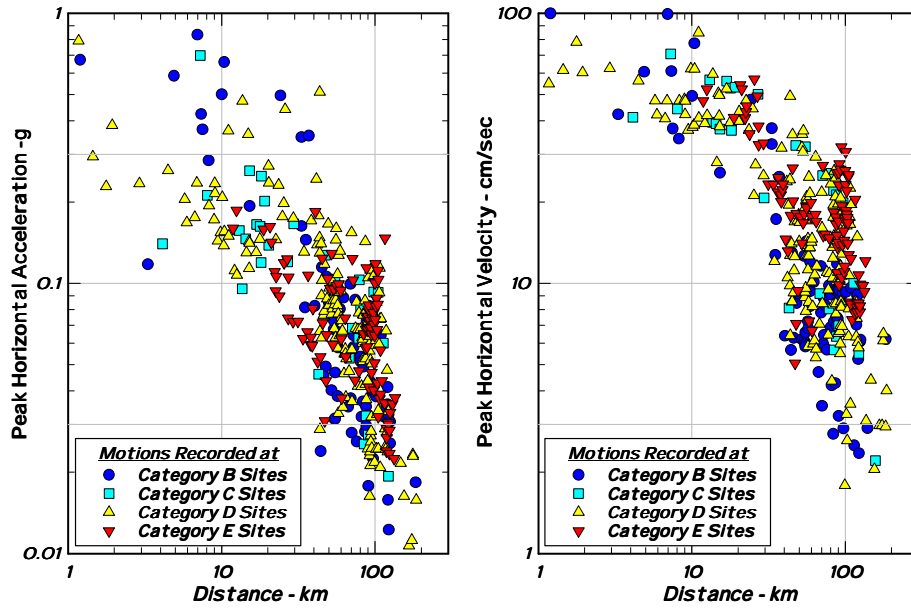


Fig. 3 Peak Horizontal Accelerations and Velocities of Motions Recorded at Various Sites during the Chi-Chi Earthquake

Peak Horizontal Accelerations and Velocities

Recorded Peak Horizontal Accelerations

The peak horizontal accelerations recorded at category B sites are shown in Fig. 4. The curve representing the derived median values using the data points for distances, R , beyond 4 km is also shown in the figure. Similar plots and curves for data recorded at Category D sites (for $R \geq 8$ km) and for Category E sites (for $R \geq 10$ km) are presented in Fig. 5 and in Fig. 6, respectively.

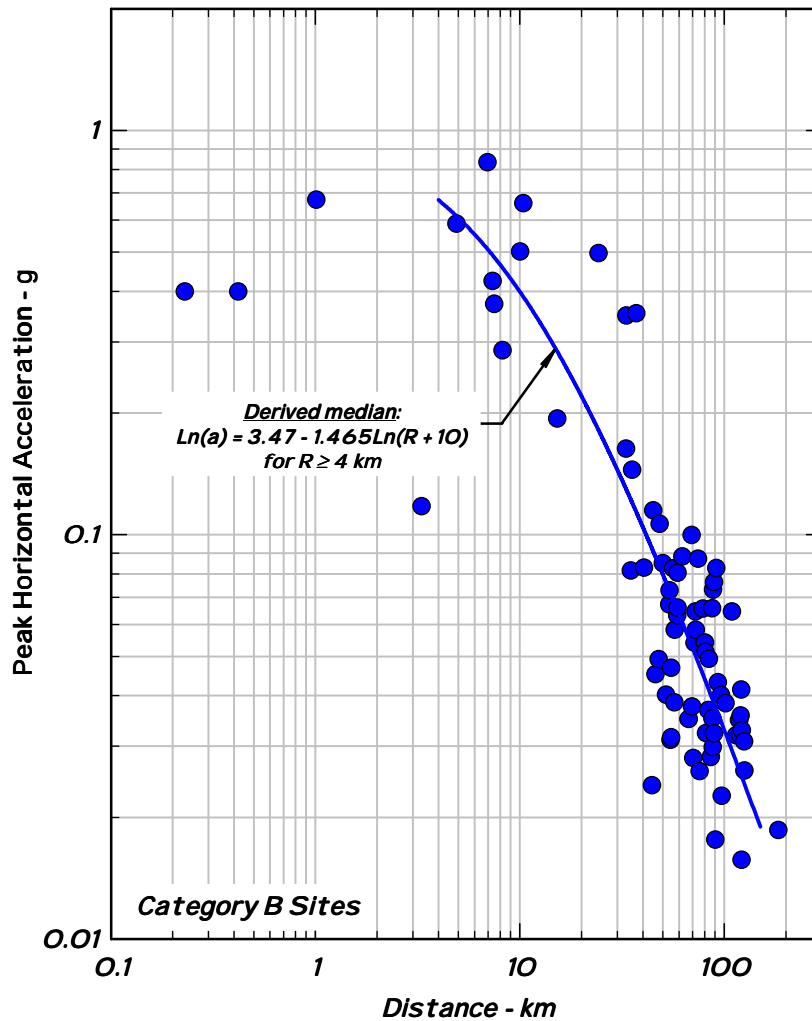


Fig. 4 Peak Horizontal Accelerations and Derived Median Curve for Motions Recorded at Category B Sites

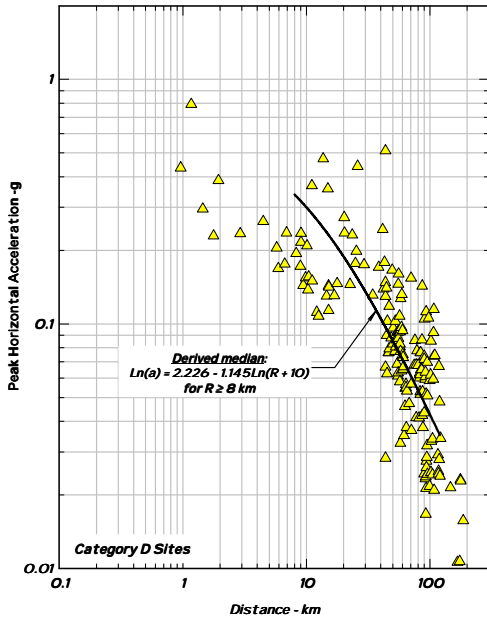


Fig. 5 Peak Horizontal Accelerations and Derived Median Curve for Motions Recorded at Category D Sites

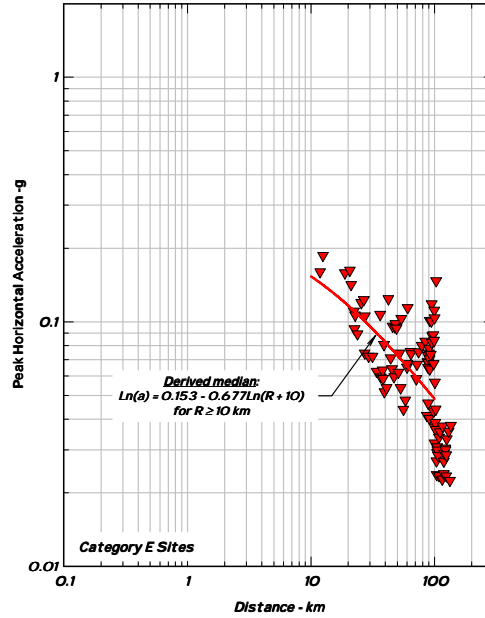


Fig. 6 Peak Horizontal Accelerations and Derived Median Curve for Motions Recorded at Category E Sites

The derived equations of the median, together with the applicable distance range, for Category B, D and E sites are listed in Table 2.

Table 2 Derived Equations for Median Peak Horizontal Acceleration for Category B, D & E Sites

Category	Applicable Distance, R	Equation for Median Acceleration, a , in g's
B	$4 \leq R \leq 150$ km	$\text{Ln}(a) = 3.470 - 1.465 \text{Ln}(R + 10)$
D	$8 \leq R \leq 120$ km	$\text{Ln}(a) = 2.226 - 1.145 \text{Ln}(R + 10)$
E	$10 \leq R \leq 100$ km	$\text{Ln}(a) = 0.153 - 0.677 \text{Ln}(R + 10)$

Influence of Local Site Conditions on Peak Horizontal Accelerations

The data shown in Figs. 3 through 6 indicate a definite influence of the local site conditions on peak horizontal accelerations. This influence is illustrated in Fig. 7, which shows the variations of peak horizontal accelerations at Category D and Category E sites in relation to the peak horizontal accelerations at Category B sites. Also shown in Fig. 7 are the variations, based on data recorded in the 1971 San Fernando earthquake, of peak horizontal accelerations obtained at deep soil sites (which are probably comparable to Category C or possibly Category D sites) in relation to peak horizontal accelerations recorded at rock or rock-like sites (which are probably comparable to Category B sites). The information presented in Fig. 7 provides the following observations:

- The median horizontal peak accelerations at Category D sites are larger than those at Category B sites for levels of shaking less than about 0.1g, but are smaller at higher levels of shaking.
- The trend obtained for deep soil sites in the 1971 San Fernando earthquake are similar to those obtained at Category D sites in the 1999 Chi-Chi earthquake.
- The median horizontal peak accelerations at Category E sites are somewhat larger than those at Category B sites for levels of shaking less than about 0.07g, but are significantly smaller at higher levels of shaking.

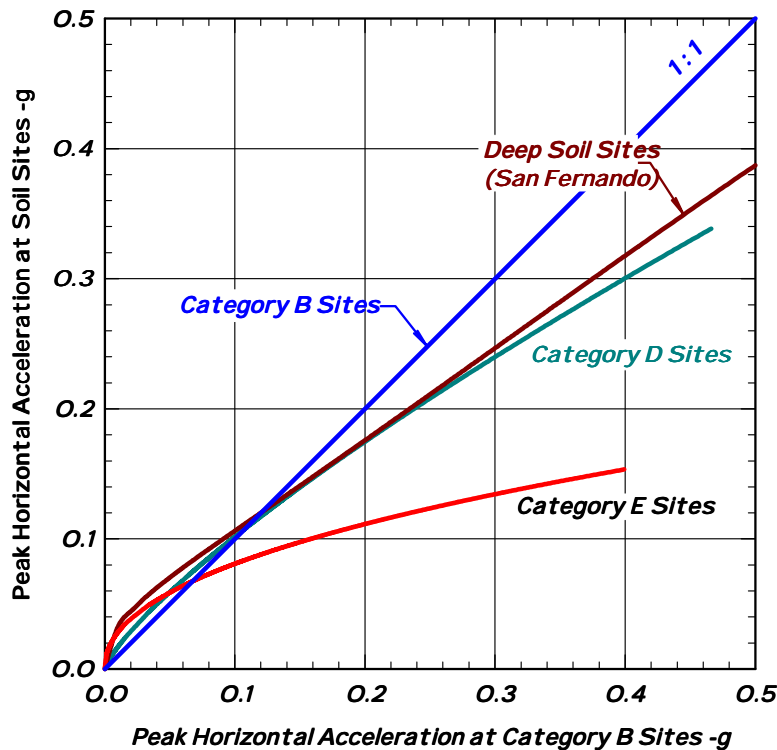


Fig. 7 Variations of Median Peak Horizontal Accelerations for Various Site Conditions with Those on Rock or Rock Like Sites

Recorded Peak Horizontal Velocities

The peak horizontal velocities recorded at category B sites are shown in Fig. 8. The curve representing the derived median values using the data points for distances, R , beyond 4 km is also shown in the figure. Similar curves for data recorded at Category D sites and for Category E sites were obtained. The derived equations of the median velocity, together with the applicable distance range, for Category B, D and E sites are listed in Table 3.

Table 3 Derived Equations for Median Peak Horizontal Velocity for Category B, D & E Sites

Category	Applicable Distance, R	Equation for Median Velocity, v , in cm/sec
B	$4 \leq R \leq 150$ km	$Ln(v) = 6.465 - 1.012 Ln(R + 5)$
D	$8 \leq R \leq 120$ km	$Ln(v) = 6.421 - 0.909 Ln(R + 5)$
E	$10 \leq R \leq 100$ km	$Ln(v) = 6.149 - 0.736 Ln(R + 5)$

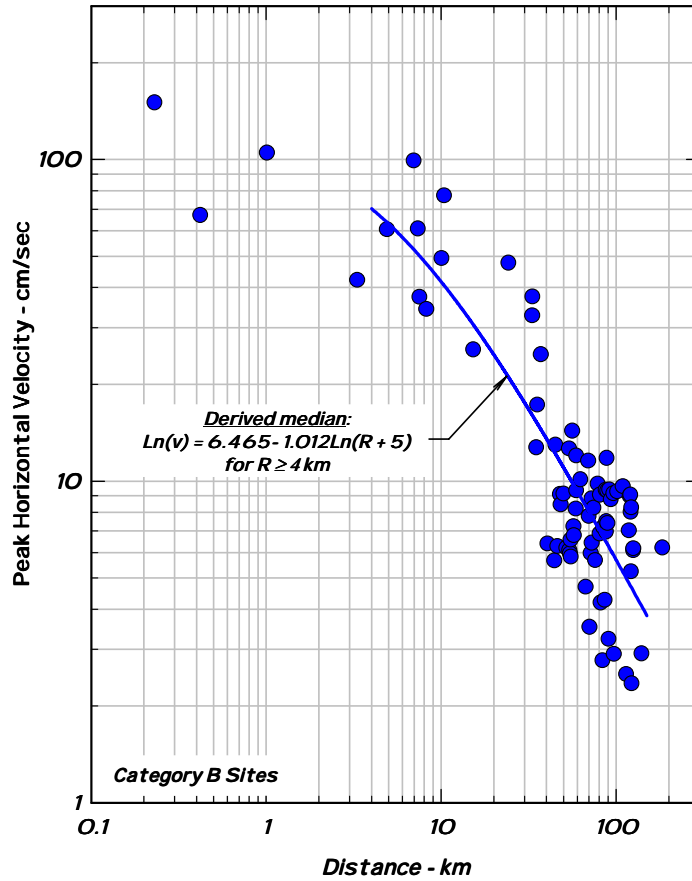


Fig. 8 Peak Horizontal Velocities and Derived Median Curve for Motions Recorded at Category B Sites

Influence of Local Site Conditions on Peak Horizontal Velocities

The data shown in Fig. 3 indicate a definite influence of the local site conditions on peak horizontal velocities. This influence is illustrated in Fig. 9, which shows the variations of peak horizontal velocities at Category D and Category E sites in relation to the peak horizontal velocities at Category B sites. The information presented in Fig. 9 provides the following observations:

- The median horizontal peak velocities at Category D sites are larger than those at Category B sites for all levels of shaking.
- The median horizontal peak velocities at Category E sites are larger than those at both Category B and Category D sites for all levels of shaking.

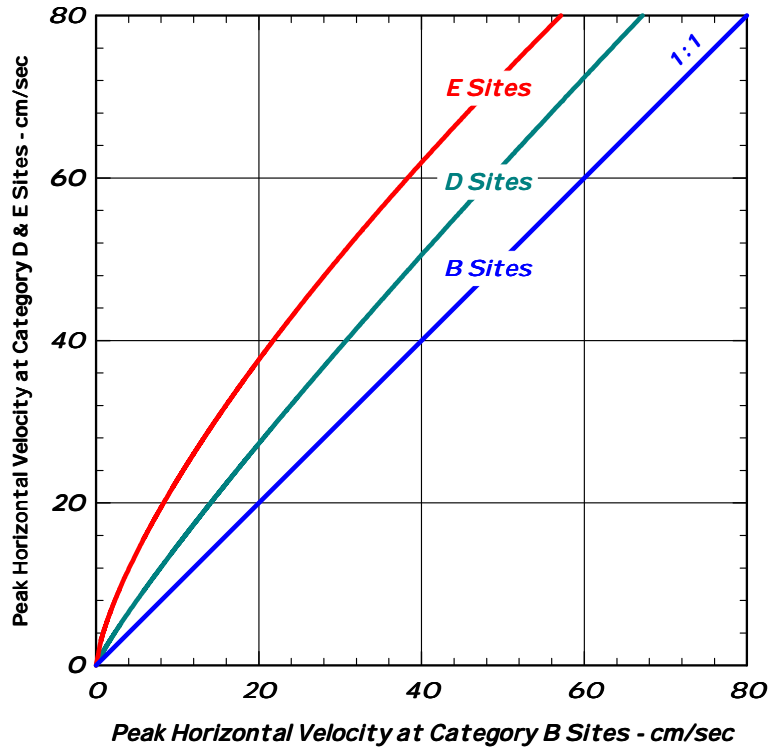


Fig. 9 Variations of Median Peak Horizontal Velocities at Category D and E Sites with Those at Category B Sites

Spectral Shapes

The spectral ordinates for a selected number of recordings at Category B sites were examined to evaluate the influence of the level of shaking on the spectral shape, i.e., plot of the spectral acceleration divided by the zero period acceleration (zpa) versus period. Recordings at the Stations listed in Table 4 were used for this purpose. The average spectra for each set are shown in Fig. 10; note that the average zpa for each set was rounded to the nearest 0.1g.

The spectral shapes shown in Fig. 10 indicate a significant shift in the frequency content toward the longer periods (lower frequencies) as the level of shaking increases. This trend is suggestive of nonlinear behavior of the strata underlying the recording stations. It will be necessary to investigate the subsurface conditions at these stations to fully assess the trends shown in Fig. 10.

The spectral shape for average zpa of 0.3g shown in Fig. 10 for Category B sites is compared in Fig. 11 to the spectral shape obtained for Category D Stations, whose average acceleration is also about 0.3g. The Category D Stations used are listed in Table 5. The results shown in Fig. 11 are indicative of the softer nature of category D sites compared to category B sites.

Table 4 Records Used for Obtaining Spectral Shapes
Category B Sites

Set No.	Station	Zero Period Acceleration (zpa) - g	Average zpa for the Set - g
1	CHY080	0.833	0.712
	TCU065	0.674	
	TCU084	0.660	
2	TCU052	0.399	0.398
	TCU067	0.399	
	TCU072	0.424	
	TCU078	0.372	
3	NST	0.353	0.327
	TCU047	0.348	
	TCU089	0.286	

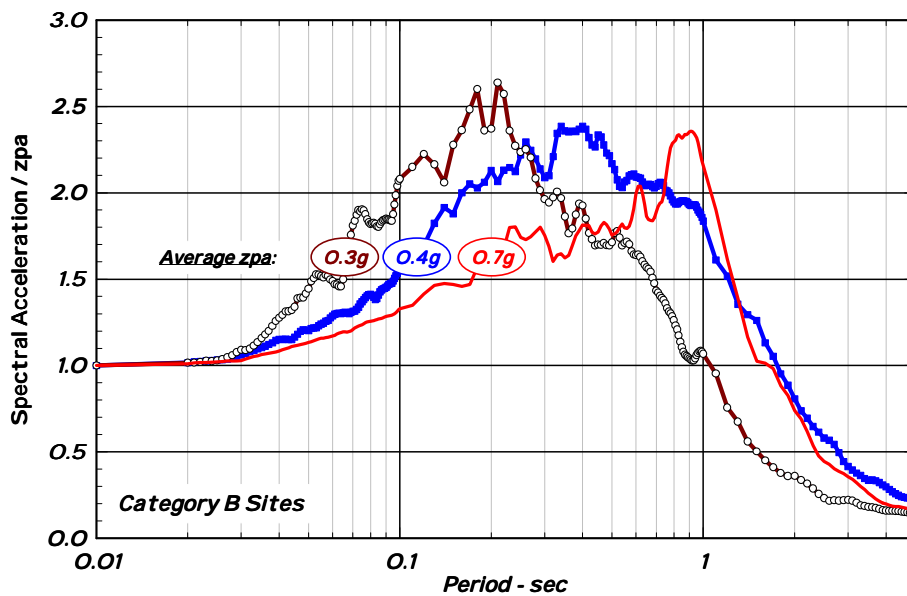


Fig. 10 Variations of Spectral Shapes with Level of Shaking for Motions Recorded at Category B Sites

Table 5 Records Used for Obtaining Spectral Shapes
Category D Sites

Station	Zero Period Acceleration (zpa) - g	Average zpa for the Set - g
CHY006	0.357	0.32
CHY034	0.273	
CHY101	0.368	
TCU049	0.262	
TCU075	0.295	
TCU076	0.386	

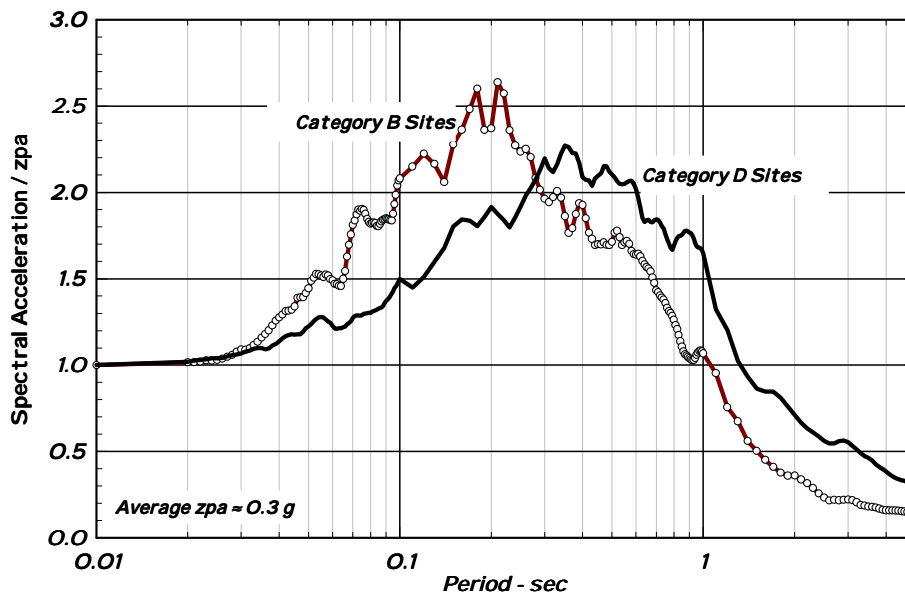


Fig. 11 Comparison of Spectral Shapes for Motions Recorded at Category B and at Category D Sites with Average $z_{pa} \approx 0.3g$

Comparison With Spectral Shapes for Recordings from the 1994 Northridge Earthquake

The spectral shapes for motions recorded at deep soil sites in the 1994 Northridge earthquake also provided similar trends to those discussed above for the motions recorded at Category B sites in the Chi-Chi earthquake. The spectral shapes for the Northridge motions are presented in the top part of Fig. 12. The middle and the lower parts of Fig. 12 show comparisons of the spectral shapes for the Northridge and the Chi-Chi motions at comparable levels of shaking.

The middle part of Fig. 12 shows this comparison at a $z_{pa} \approx 0.3g$; the two spectral shapes are almost identical. The lower part of the figure shows this comparison at a $z_{pa} \approx 0.7g$; the two spectral shapes are similar but are distinctly different over a significant period range. Once the subsurface conditions at the Chi-Chi sites are ascertained more fully (by drilling and measurement of shear wave velocities) it will be possible to examine the similarities and the differences shown in Fig. 12.

Comparison of Recorded Peak Horizontal Accelerations with Attenuation Relationships Derived Prior to the Chi-Chi Earthquake

The peak horizontal accelerations of the motions recorded at Category B sites were compared to those calculated using the attenuation relationship by Abrahamson and Silva (1997) and the attenuation relationship by Idriss (1999). Both relationships had been derived prior to the Chi-Chi earthquake. The majority of the data used to derive these attenuation relationships were recorded in California.

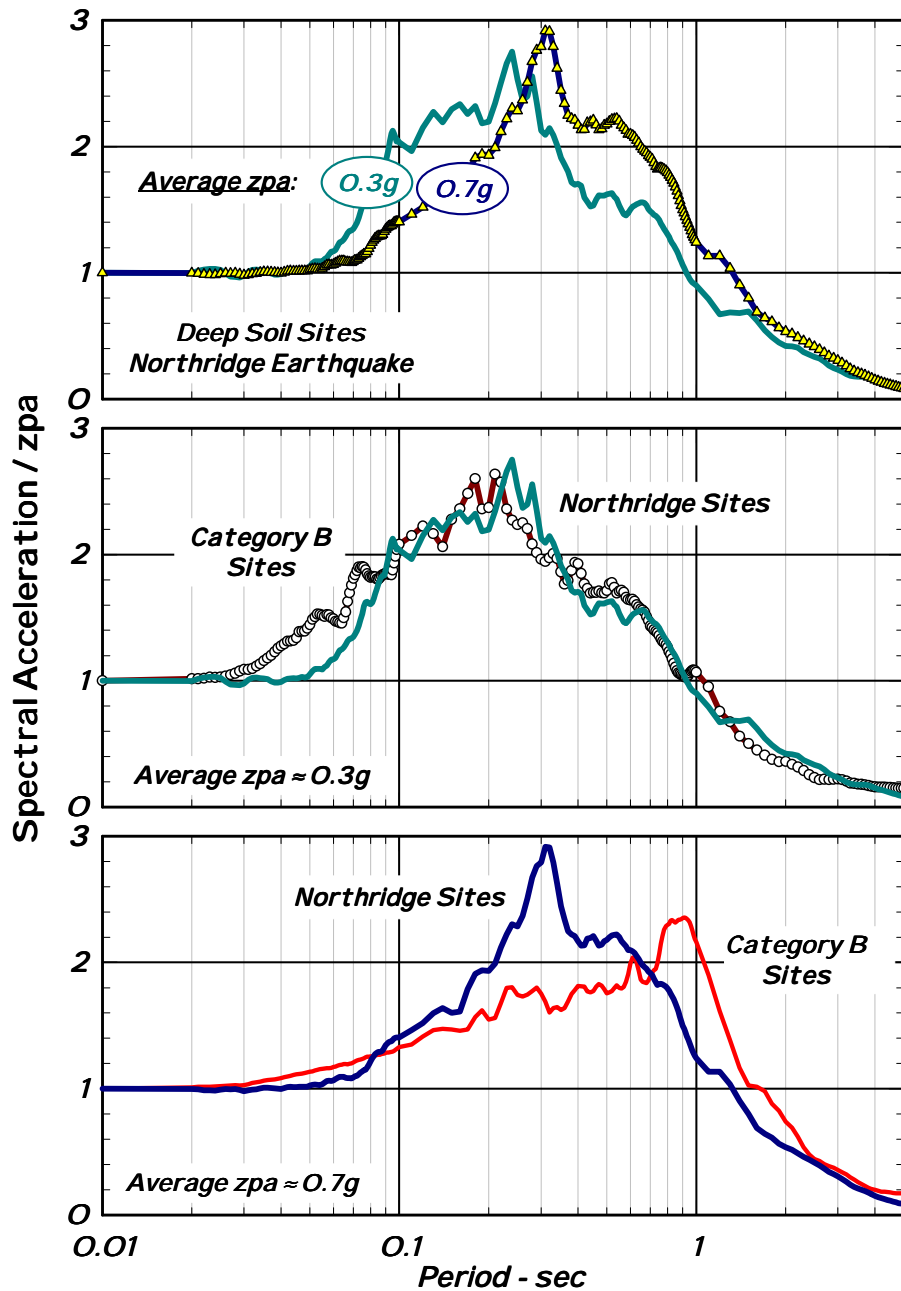


Fig. 12 Spectral Shapes for Motions Recorded at Deep Soil Sites in the 1994 Northridge Earthquake and Comparison of these Spectral Shapes with Corresponding Shapes for Motions Recorded at Category B Sites in the Chi-Chi Earthquake

The equation derived by Abrahamson and Silva for calculating the median peak horizontal accelerations for a magnitude 7.6 earthquake occurring on a reverse source (but excluding the hanging wall effect) is given below:

$$\ln(a) = 1.7272 - 0.941 \ln(\sqrt{R^2 + 5.6^2})$$

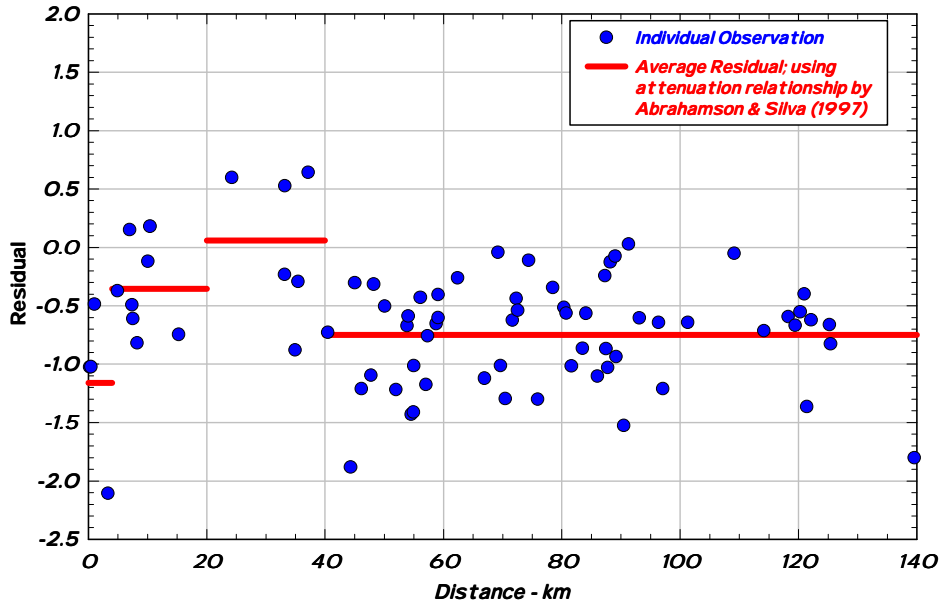


Fig. 13 Residuals Calculated Using Attenuation Relationship by Abrahamson & Silva (1997) – Category B Sites

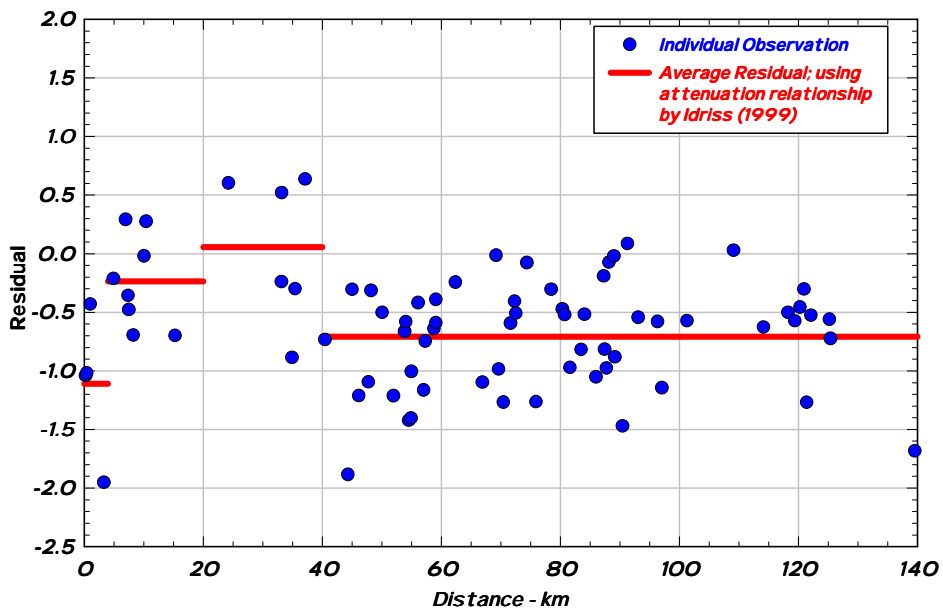


Fig. 14 Residuals Calculated Using Attenuation Relationship by Idriss (1999) – Category B Sites

The equation derived by Idriss for calculating the median peak horizontal accelerations for a magnitude 7.6 earthquake occurring on a reverse source is given below:

$$\ln(a) = 2.8612 - 1.1782 \ln(R + 10)$$

In both equations, a is the peak horizontal acceleration (geometric mean of the two horizontal components), and R is the closest distance to the rupture surface.

These equations were used to calculate the estimated peak horizontal acceleration at each Category B site and hence the corresponding residual. The residuals obtained using the attenuation relationship by Abrahamson and Silva are presented in Fig. 13 and those obtained using the attenuation relationship by Idriss are presented in Fig. 14. The average residual over selected distance ranges are also shown in each figure. The results shown in Figs. 13 and 14 offer the following observations:

- The two attenuation relationships provide almost the same results for this event, with the relationship by Abrahamson and Silva being slightly more conservative.
- The peak horizontal accelerations recorded in this earthquake, at distances less than about 4 km from the rupture surface, are about 30% of those calculated using the attenuation relationships that had been derived prior to this earthquake.
- The recorded accelerations, at distances ranging from about 4 to 20 km, are about 70% of the calculated values.
- The recorded accelerations, at distances ranging from about 20 to 40 km, are almost identical to the calculated values.
- The recorded accelerations, at distances beyond about 40 km, are about 50% of the calculated values.

The recordings obtained in the larger aftershocks need to also be examined to provide further information about the differences in the motions recorded during the Chi-Chi earthquake and those obtained in other earthquakes.

Summary and Conclusions

The earthquake ground motions recorded during this earthquake were examined in terms of the peak horizontal accelerations and peak horizontal velocities recorded at three generalized site conditions. The data suggest a dependence of these parameters on local site conditions; this dependence appears similar to that observed in previous earthquakes, such as the 1971 San Fernando earthquake.

Examination of the spectral shapes at the stiffest site category indicates that these sites exhibit nonlinear behavior at the levels of shaking examined (0.3g, 0.4g and 0.7g). The trends observed in the Chi-Chi earthquake are similar to those that had been observed in the 1994 Northridge earthquake.

The peak horizontal accelerations recorded in this earthquake were compared to those calculated using attenuation relationships that had been derived prior to this earthquake. The results of these comparisons (in terms of residuals) indicate that the values recorded during the Chi-Chi earthquake are: (i) about 30% of the calculated values at distances less than about 4 km from the rupture surface; (ii) about 70% of the calculated values at distances ranging from about 4 to 20 km; (iii) almost identical to the calculated values at distances ranging from about 20 to 40 km; and (iv) about 50% of the calculated values at distances larger than about 40 km.

These preliminary findings suggest the strong need to fully investigate the subsurface conditions at as many of the recordings stations as possible to finalize the site categories and to confirm or modify the findings reached based on these preliminary examinations of the available data. The recordings obtained in the larger aftershocks need to also be examined to provide further information about the differences in the motions recorded during the Chi-Chi earthquake and those obtained in other earthquakes.

Acknowledgements

We thank our colleagues in Taiwan for their cooperation in our efforts to examine the effects of the earthquake and in providing, in a timely manner, the strong motion recordings for the main shock of the Chi-Chi earthquake. Shyh-Jeng Chiou of Geomatrix, San Francisco, provided the site categories and site classification information and translated the descriptions of the site categories into English. His assistance in this effort is gratefully acknowledged.

References

Abrahamson, N. A. and Silva, W. J. (1997) "Empirical Response Spectral Attenuation Relations for Shallow Crustal Earthquakes", *Seismological Research Letters*, Vol. 68, No. 1, January / February 1997, pp 94-127.

Cheng, Thomas and Lee, C. T. (2000) "Site Categories at Strong Motion Stations", National Central University; document prepared in Chinese and translated by Shyh-Jeng Chiou of Geomatrix.

Idriss, I. M. (1999) "Geotechnical Considerations for Evaluating Seismic Effects on Transportation Structures", Presentation Notes, International Workshop on Mitigation of Seismic Effects on Transportation Structures, NCREC, Taipei, Taiwan, July 12 – 14, 1999.

Lee, W. H. K., Shin, T. C., Kuo, K. W., and Chen, K. C. (1999) "CWB Free-Field Strong Motion data from the 921 Chi-Chi Earthquake: Volume 1. Digital Acceleration Files on CD-ROM", Seismology Center, Central Weather Bureau, Taipei, Taiwan, December 6, 1999.